



Contents lists available at ScienceDirect

Journal of King Saud University – Science

journal homepage: www.sciencedirect.com

Effect of calcination temperature on structural and magnetic properties in cobalt ferrite nano particles

Budi Purnama^{a,*}, Agung Tri Wijayanta^b, Suharyana^a

^a Department of Physics, Faculty of Mathematics and Natural Science, Sebelas Maret University, Jl. Ir. Sutami 36A, Surakarta 57126, Indonesia

^b Department of Mechanical Engineering, Faculty of Engineering, Sebelas Maret University, Jl. Ir. Sutami 36A, Surakarta 57126, Indonesia

ARTICLE INFO

Article history:

Received 11 June 2018

Accepted 30 July 2018

Available online 1 August 2018

Keywords:

Saturation magnetisation

Cobalt ferrite nanoparticles

Compact granules

ABSTRACT

We discuss the calcination temperature dependence of the structural and magnetic properties of co-precipitated cobalt ferrite. Calcination process was performed under atmospheric condition without inert gas. High-purity cobalt ferrite nanoparticles are obtained experimentally. The size of the crystallites increases with the increase of the calcination temperature. Furthermore, the XRD analysis result show that cation redistribution occurs with the increase of the calcination temperature. The SEM result show that the structural organization of these particles changes from separate nanoparticles to the formation of compact granules with increasing calcination temperature. As a result, the saturation magnetization increases with the calcination temperature, reaching up to 62.30 emu/g. It was found that the cation distribution for both tetrahedral and octahedral sites affected by the calcination temperature.

© 2018 Production and hosting by Elsevier B.V. on behalf of King Saud University. This is an open access article under the CC BY-NC-ND license (<http://creativecommons.org/licenses/by-nc-nd/4.0/>).

1. Introduction

In the last decade, there has been great interest in cobalt ferrite nanoparticles with regard to their potential industrial and medical applications. Moderate magnetic saturation, high coercivity, chemical stability, and good mechanical strength are the reasons for the wide applications of this cobalt ferrite nanoparticles (Kotnala and Shah, 2015). Indeed, the magnetic characteristics of cobalt ferrite nanoparticles can be modulated by heat treatment (Huixia et al., 2014; Nlebedim et al., 2014; Swatsitang et al., 2016; Prabhakaran et al., 2017a,b) including vacuum annealing Bhowmik et al. (2015), pH solution (Safi et al., 2015; Huang et al., 2016), synthesis temperature (Hutamaningtyas et al., 2016; Prabhakaran et al., 2017a,b) or by the substitution with other metal ions such as Ti (Nlebedim and Jiles, 2015; Monaji et al., 2017), Al (Zaki et al., 2015; Maurya et al., 2016), Zn (He, 2012; Manikandan et al., 2014; Yadav et al., 2015; Huang et al., 2016), Mo (Heiba et al., 2014), Ni (He, 2013; Mahmoud et al., 2014), Sulphur

Cao et al. (2016), rare earth metals such as Zr (Monaji et al., 2017), Sr (Kumar and Kar, 2016; El-Ghazzawy and Amer, 2017; Lima et al., 2015; Shirsath et al., 2016; Tang et al., 2016, 2017) and others. In addition, the increased saturation magnetization contributes to the surface and inter-particle interactions between the cobalt and iron ions in the crystalline structure (Saidani et al., 2015). Furthermore, the magnetic characteristics of the cobalt ferrite nanoparticles can be modified through the charge-transfer effect (Rakshit et al., 2014). The nanoparticles material has demonstrated good thermal stability, which is a main priority for high temperature applications (Franco and e Silva, 2010). The ease of modifying the magnetic properties has an opportunity to present a single domain nanoparticles which are suitable for various desired applications especially in medicine (Kotnala and Shah, 2015; Ahmad and Zhou, 2017).

From the view point of the theory, the modified magnetic properties of cobalt ferrite nanoparticles are conventionally explained by the distribution of cobalt ferrite constituent cations (Mohamed and Yehia, 2014; Liu et al., 2016; Dalal et al., 2016; Sato Turtelli et al., 2012). In the face-centered cubic spinel structure, cobalt ferrite shows its contribution in the magnetic moment of the tetrahedral sites and octahedral sites (Kotnala and Shah, 2015). Co^{2+} and Fe^{3+} cations share the typical amount cation and occupy the octahedral site in the inverse-spinel structure. Whereas the Co^{2+} ions only have a preference on the octahedral sites (Liu et al., 2016). It should be noted that the magnetic moment of Fe^{3+} is greater than that of Co^{2+} . The distribution of the competing

* Corresponding author.

E-mail address: bpurnama@mipa.uns.ac.id (B. Purnama).

Peer review under responsibility of King Saud University.



cations such as the Fe^{3+} ions occupies octahedral positions to a greater extent than Co^{2+} attributable the increase of the saturation magnetization (Nlebedim et al., 2014; Hutamaningtyas et al., 2016). In Co doped Ni–Zn ferrite, the distribution of cations occurs for both octahedral and tetrahedral sites with the increase of annealing temperature (Dalal et al., 2016). Preparation method of the cobalt ferrite nanoparticles defines the distribution of the Co^{2+} and Fe^{3+} cations in the tetrahedral and octahedral sites (Sato Turtelli et al., 2012). Cation-redistribution of cobalt ferrite nanoparticle also depends on the synthesis temperature (Hutamaningtyas et al., 2016; Prabhakaran et al., 2017a,b). In Ga substituted cobalt ferrite nanoparticles, the increase of Ga content promotes migration of Co^{2+} cation from octahedral site to tetrahedral sites (Mohamed and Yehia, 2014).

Heat treatment is a popular procedure for the redistribution of the cations studied as well as the synthesis heating procedure and post-synthesis annealing. Eventhough, the thermal energy also affects to the recombination process of granular nanoparticles. Up to now, several reported experiments considering the effect of heating, have conducted for the same of any magnitude levels only for low temperature and high temperature mainly at the condition near the Curie temperature. In other words, the final grain size is obtained from the same thermal effect which is independent to the level of temperature. Then the distribution of the cations can be directly associated with the heating treatment. Reports in published papers on heat treatment to study the structural and magnetic properties in co-precipitated cobalt ferrite are still interesting one. At the present study, the calcination temperature dependence of structural and magnetic properties in co-precipitated cobalt ferrite is investigated experimentally. Effect of heat calcination considers not only for modifying the distribution and displacement of the Co^{2+} and Fe^{3+} cations in the inverse face-centered cubic spinel, but also the change in dimensions of the primitive unit cells in granular nanoparticles. Findings will contribute to the understanding of heat treatment effect in the efforts for improving the face-centered cubic spinel arrangement of cobalt ferrite.

2. Experimental methods

Cobalt ferrite nanoparticles were synthesized using the co-precipitation method as explained previously (Purnama et al., 2015; Hutamaningtyas et al., 2016). The first step was preparing the precursor. $\text{Co}(\text{NO}_3)_2 \cdot 6\text{H}_2\text{O}$ (Merck), $\text{Fe}(\text{NO}_3)_3 \cdot 9\text{H}_2\text{O}$ (Merck) and NaOH (Merck) were used in this study without further purification. The whole glassware used in this experiment were cleaned using an ultrasonic cleaner in an alcohol environment. Then the glassware was dried by blowing ultra-high purity of nitrogen gas. Stoichiometric amount of 0.001 M $\text{Co}(\text{NO}_3)_2 \cdot 6\text{H}_2\text{O}$ (Merck), 0.002 M $\text{Fe}(\text{NO}_3)_3 \cdot 9\text{H}_2\text{O}$ (Merck) were dissolved in distilled water under stirring of 250 rpm until homogenous. The stirring process performed at room temperature. The obtained solution was then added drop wise to 100 ml of 4.8 M NaOH. During titration, the NaOH solution was stirred at 1000 rpm and temperature was kept at 95 °C then continually stirred for 2 h. After cooling to room temperature, the precipitate was repeatedly washed with distilled water so that the cleanliness of the precipitate product was attained. In order to remove residual water, the product was dried overnight in an oven at 100 °C. Thereafter, the product was annealed at 600 °C, 800 °C and 1000 °C for six hours at air condition. X-ray diffraction using a Bruker D8 Advance system was used to determine the crystalline structures of the final samples. The morphology of the magnetic nanoparticles was observed using SEM (FEI type Inspect 21). Their magnetic properties were evaluated using VSM (Oxford VSM 1.2H)

3. Results and discussions

Fig. 1 presents a typical TG/DTA curve of co-precipitated cobalt ferrite nanoparticles from room temperature to 1000 °C. The curve gradation indicates the relative change in the sample mass. In the first gradation, between RT and 340 °C, a relative mass loss of 3% was observed, which is attributed to hydrocarbon waste including dehydration and then loss of adsorbed water following decarbonation (Ajroudi et al., 2014; Purnama et al., 2015). In this interval, the decarbonation process of nanoparticles cobalt ferrite indicated with a peak of exothermal i.e. at temperature of 230 °C with heat flow of 27.3 mW. Between 340 °C and 530 °C, a relative mass loss of 0.3% was observed. This is associated with the nanoparticle dislocation process towards a stable configuration. A final plateau was observed from 530 °C to 900 °C, where the samples do not experience additional mass loss. Heat flow supplied by the heating process at temperatures above 530 °C is considered to be used for crystallization (Zhao et al., 2008). Here, the change of nano granular type in cobalt ferrite is expected to occur when the crystallization process takes place.

The X-ray diffraction patterns of the cobalt ferrite nanoparticles at the three calcination temperatures (600 °C, 800 °C and 1000 °C) under atmospheric conditions for six hours holding time are depicted in Fig. 2. They are closely resembled the standard crystalline structure of CoFe_2O_4 from the International Centre for Diffraction Data (ICDD) number 221086, which belongs to the face-centered cubic spinel type (Fd-3m). There were no characteristic peaks that indicate the presence of un-expected oxides or other impurities in the sample. The crystallite size D is calculated by a Scherrer formula, $D = \frac{0.9\lambda}{\rho \cos\theta}$ at the strongest peak, the peak intensity ratio I_{220}/I_{222} and I_{220}/I_{422} is presented in Table 1. The sample annealed at 800 °C exhibits the highest intensity in comparison with the other samples. Using the strongest XRD peak and the Scherer formula, the crystallite sizes of 31.74, 35.28 and 42.62 nm were obtained for the cobalt ferrite nanoparticles, which correspond to the calcination temperatures of 600 °C, 800 °C and 1000 °C, respectively.

Furthermore, the results XRD peak intensity I_{220}/I_{222} and I_{220}/I_{422} show the distribution of cations in octahedral and tetrahedral sites, respectively. The XRD peak intensity ratios for both I_{220}/I_{222} and I_{220}/I_{422} obtain 0.81 and 3.36, respectively, for the temperature calcination of 600 °C. For the temperature calcination of 800 °C, the

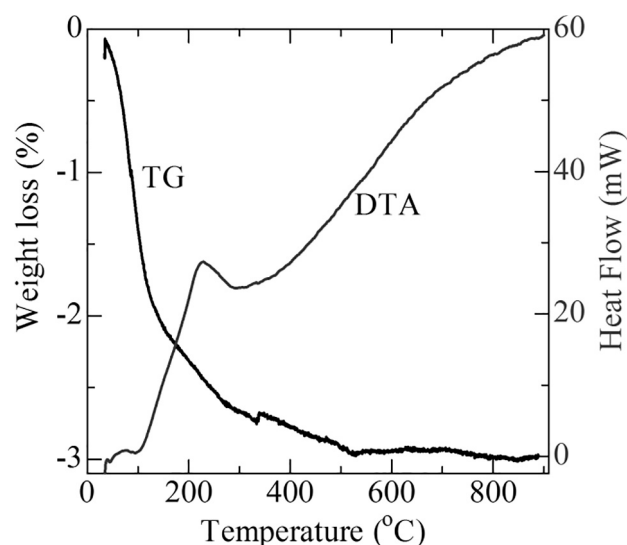


Fig. 1. Typical TG/DTA of cobalt ferrite nanoparticle synthesised using the co-precipitation method.

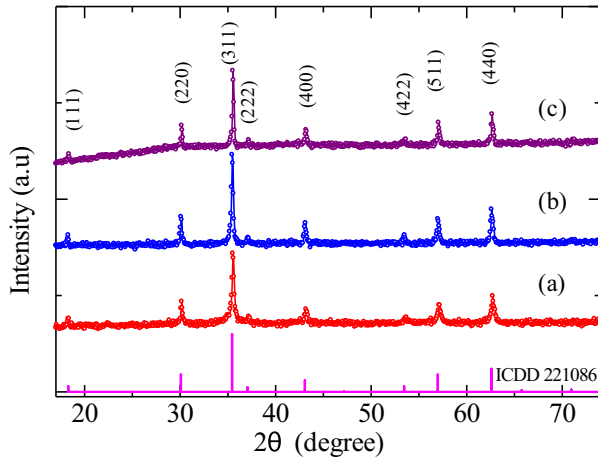


Fig. 2. X-ray diffraction patterns for cobalt ferrite nanoparticles at three calcination temperatures, namely (a) 600 °C, (b) 800 °C and (c) 1000 °C, for six hours holding time.

Table 1

Crystallite size, the XRD peak ratio I_{220}/I_{222} , I_{422}/I_{222} and saturated magnetization for cobalt ferrite nano particles sample at temperatures calcination of 600 °C, 800 °C and 1000 °C.

| | Temperature Calcination (for 6 h @ air condition) | | |
|---------------------------|---|--------|---------|
| | 600 °C | 800 °C | 1000 °C |
| Crystallite size D (nm) | 31.74 | 35.29 | 42.62 |
| Lattice parameter a (Å) | 8.37 | 8.38 | 8.37 |
| I_{220}/I_{222} | 3.36 | 3.92 | 4.29 |
| I_{422}/I_{222} | 0.81 | 1.27 | 1.34 |
| M_s (emu/g) | 38.58 | 53.59 | 62.30 |
| H_c (Oe) | 614 | 877 | 641 |

ratio of both I_{220}/I_{222} and I_{220}/I_{422} change to 3.92 and 1.27. Then the I_{220}/I_{222} and I_{220}/I_{422} provide 4.29 and 1.34 when the temperature calcination of 1000 °C. The experimental results for 1000 °C offers very close to the numerical calculated results i.e. I_{220}/I_{222} is equal 4.1 and I_{220}/I_{422} is 1.3 where Co^{2+} and Fe^{3+} completely separate at tetrahedral and octahedral sites (Ajroudi et al., 2014). The modification of the peak XRD intensity ratio indicates that the calcination temperature affected cation distribution for both tetrahedral and octahedral sites. The occurrence of the cation distribution should change the magnetic properties of the cobalt ferrite nanoparticles.

Fig. 3 depicts the SEM images of the cobalt ferrite nanoparticles applying a 150,000 \times magnification at the above calcination temperatures. The observed particle distribution indicated by a small circle was the typical appearance for cobalt ferrite nanoparticles. A particles size distribution was analyzed by using WSxM software (Horcas et al., 2007). The results indicate that the average particle sizes are comparable to the calculation of crystallites' size D obtained by the Scherrer method at the highest peak. The typical SEM results for in granular nanoparticles provided a reasonable fit with the results reported by Avazpour et al. (2015) and Kefeni et al. (2017). In addition, it is clearly observed that the nanoparticle organization changes from single particles separate from one another (calcination temperature at 600 °C and 800 °C, see Fig. 3 (a) and (b)) to compact nanoparticle granules (calcination temperature at 1000 °C, see Fig. 3(c)). At the calcination temperature of 800 °C, it is approximately 50.95% (=800/1570) of the cobalt ferrite melting point (1570 °C), whereas 1000 °C corresponds to approximately 63.69% (=1000/1570) of the melting point temperature. Therefore, the heat energy from the temperature calcination is used by the nanoparticles to conglomerate and then diffuse in order to form larger granular particles and for a greater distribution. Nevertheless, the lattice parameters a is almost unchanged i.e. 8.37 Å, 8.38 Å and 8.37 Å for the temperature calcination of 600 °C, 800 °C and 1000 °C respectively. Here, the transitional temperature is estimated to be approximately about 63% of the melting point. This present experimental result related to the melting point offers a good contribution of heat treatment that has not yet been reported (Avazpour et al., 2015; Kefeni et al., 2017).

Fig. 4 presents the hysteresis curve for cobalt ferrite nanoparticle samples at the three different calcination temperatures. Calculation data of the hysteresis graph i.e. saturated magnetization M_s and coercive field H_c present at Table 1. There is a significant difference in the saturation magnetization. The sample corresponding to the lower calcination temperature (600 °C) had a saturation magnetization (M_s) value of 38.58 emu/g. The samples corresponding to higher calcination temperatures of 800 °C and 1000 °C had M_s values of 53.59 emu/g and 62.30 emu/g, respectively. The increase of the M_s with the increase of the temperature calcination can be attribute to the cations redistribution that expected at previous discussion where the Fe^{3+} ions indicate migrate to octahedral sites with the increase of calcination temperature. The preference of the net magnetic moment of cobalt ferrite nano particles with the spinel structure are presented as (Niebedim and Jiles, 2015): $m = \sum m_{\text{octahedral}} - \sum m_{\text{tetrahedral}}$. It should be noted that the magnetic moment of Fe^{3+} ions is greater than that of Co^{2+} ions. So that the dominantly redistribution of Fe^{3+} ions at octahedral sites will increase the total number of the magnetic moment which appears

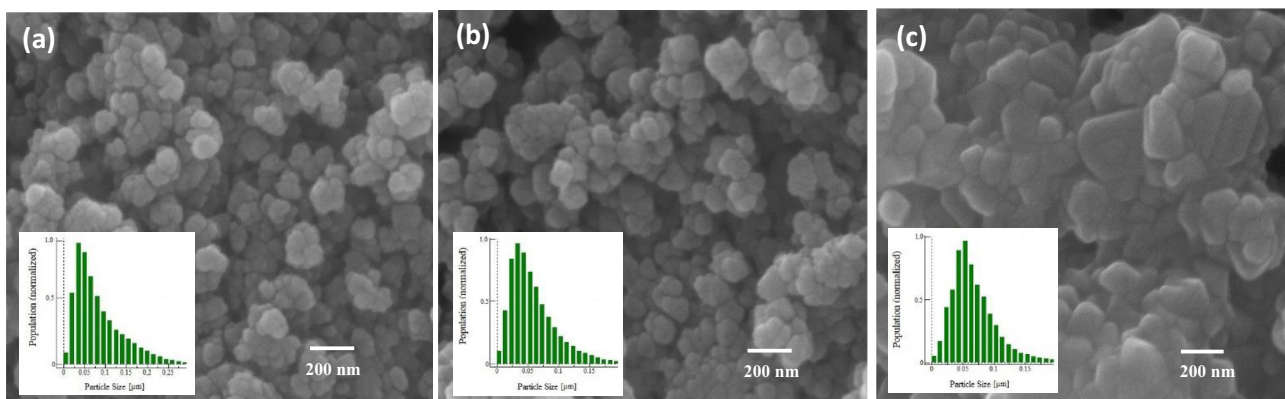


Fig. 3. Typical SEM images and particles size distribution analysis (inset) for cobalt ferrite after calcination for six hours under three different temperatures: (a) 600 °C, (b) 800 °C and (c) 1000 °C.

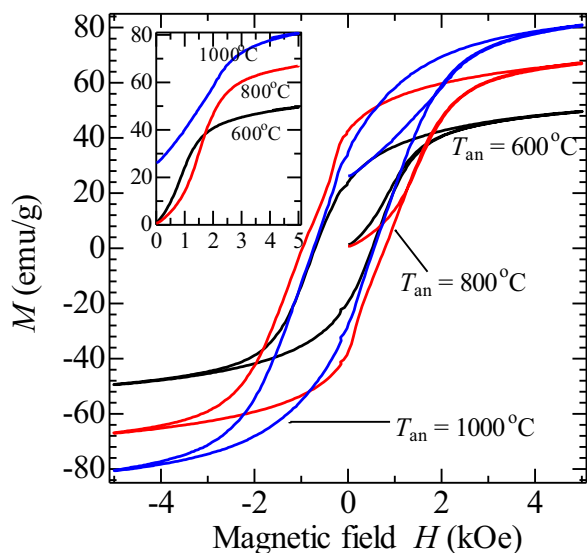


Fig. 4. A typical hysteresis curve for co-precipitated cobalt ferrite nanoparticles at the three different calcination temperatures (600 °C, 800 °C and 1000 °C). The magnetisation step from the initial magnetized state (cobalt ferrite nano-magnetic particles) to saturated magnetisation, when a magnetic field of 5000 Oe is applied (Inset).

as the increase of the saturated magnetization in the cobalt ferrite nanoparticles.

Furthermore, an interesting result is observed for the magnetization step from the initial magnetized state to the saturated magnetization state, when a magnetic field of 5 kOe was applied. Cobalt ferrite nanoparticle samples annealed at 600 °C and 800 °C present an initial magnetization state equal to zero, indicating a multi-domain magnetic configuration. With regard to the competing cations, Co^{2+} and Fe^{3+} , for the octahedral site, a final contribution of Co^{2+} and Fe^{3+} cations offers a magnetized state configuration of magnetic moments within the zero initial magnetized state. In contrast, for the high calcination temperature (1000 °C), the initial magnetized state is not zero. Thus, a single-domain magnetic configuration is suggested for as-produced samples. Redistributed Fe^{3+} cations, due to the calcination temperature, occupy an available octahedral vacancy site instead of the Co ion.

Due to the limit size for single domain realization, nanoparticles cobalt ferrite owing crystallite size is smaller than 70 nm (Berkowitz and Schuele, 1959). However, in the recent study, it is smaller than 45 (Maaz et al., 2007) and should be in single domain form. Here, a high coercive field should be attained at critical size. Then the coercive field decrease with the increase of crystallite size, where multi domain configuration realize. The high-enough coercive fields for this cobalt ferrite precipitated product with calcination temperature of 600 °C and 800 °C are 614 and 877 Oe respectively. Pinning of the magnetic domain at the interface may attribute the increase of the coercive field (Lima et al., 2015). Then the coercive field of 641 Oe is attained for the calcination temperature of 1000 °C. The reduce in coercivity compared with the sample annealed at 800 °C is associated to the change in form of nanoparticles, i.e. from separate single particles to compact nanoparticle granules.

4. Summary

The calcination temperature dependence of the structural and magnetic properties in co-precipitated cobalt ferrite is presented in this paper. The calcination procedure was performed under

atmospheric conditions without adding inert gas, producing highly pure cobalt ferrite nanoparticles. With increasing calcination temperature, the cobalt ferrite particles are conglomerated to form compact granules. Depending on calcination temperature, the domain configuration is attained for forming the crystallite size. Finally, the saturation magnetization increases with the calcination temperature by mean redistribution of the Fe cation to occupy the octahedral site to a greater extent than Co. From the present study, it means that heat treatment is one method to affect the saturation magnetization and rearrange the structure of cobalt ferrite.

Acknowledgements

This research was funded by Direktorat Riset dan Pengabdian Masyarakat Direktorat Jenderal Penguatan Riset dan Pengembangan Kementerian Riset, Teknologi, dan Pendidikan Tinggi, Indonesia contract No. 089/SP2H/LT/DRPM/2018.

References

- Ahmad, F., Zhou, Y., 2017. Pitfalls and challenges in nanotoxicology: a case of cobalt ferrite (CoFe_2O_4) nanocomposites. *Chem. Res. Toxicol.* 30 (2), 492–507. <https://doi.org/10.1021/acs.chemrestox.6b00377>.
- Ajrouti, L., Mliki, N., Bessais, L., Madigou, V., Villain, S., Leroux, C., 2014. Magnetic, electric and thermal properties of cobalt ferrite nanoparticles. *Mater. Res. Bull.* 59, 49–58. <https://doi.org/10.1016/j.materresbull.2014.06.029>.
- Avazpour, L., Toroghinejad, M.R., Shokrollahi, H., 2015. Synthesis of single-phase cobalt ferrite nanoparticles via a novel EDTA/EG precursor-based route and their magnetic properties. *J. Alloys Compd.* 637, 497–503. <https://doi.org/10.1016/j.jallcom.2015.03.041>.
- Berkowitz, A.E., Schuele, W.J., 1959. Magnetic properties of some ferrite micropowders. *J. Appl. Phys.* 30 (4), S134–S135. <https://doi.org/10.1063/1.2185853>.
- Bhowmik, R.N., Panda, M.R., Yusuf, S.M., Mukadam, M.D., Sinha, A.K., 2015. Structural phase change in $\text{Co}_{2.25}\text{Fe}_{0.75}\text{O}_4$ spinel oxide by vacuum annealing and role of coexisting CoO phase on magnetic properties. *J. Alloys Compd.* 646, 161–169. <https://doi.org/10.1016/j.jallcom.2015.05.276>.
- Cao, D., Wang, X., Pan, L., Li, H., Jing, P., Wang, J., Liu, Q., 2016. Nonmetal sulfur-doped coral-like cobalt ferrite nanoparticles with enhanced magnetic properties. *J. Mater. Chem. C* 4 (5), 951–957. <https://doi.org/10.1039/c5tc02931g>.
- Dalal, M., Mallick, A., Mahapatra, A.S., Mitra, A., Das, A., Das, D., Chakrabarti, P.K., 2016. Effect of cation distribution on the magnetic and hyperfine behaviour of nanocrystalline Co doped Ni–Zn ferrite ($\text{Ni}_{0.4}\text{Zn}_{0.4}\text{Co}_{0.2}\text{Fe}_2\text{O}_4$). *Mater. Res. Bull.* 76, 389–401. <https://doi.org/10.1016/j.materresbull.2015.12.028>.
- El-Ghazzawy, E.H., Amer, M.A., 2017. Structural, elastic and magnetic studies of the as-synthesized $\text{Co}_{1-x}\text{Sr}_x\text{Fe}_2\text{O}_4$ nanoparticles. *J. Alloys Compd.* 690, 293–303. <https://doi.org/10.1016/j.jallcom.2016.08.135>.
- Franco, A., e Silva, F. C., 2010. High temperature magnetic properties of cobalt ferrite nanoparticles. *Appl. Phys. Lett.* 96, (17). <https://doi.org/10.1063/1.3422478>
- He, H.Y., 2012. Synthesis and magnetic properties of $\text{Co}_{0.5}\text{Zn}_{0.5}\text{Fe}_2\text{O}_4$ nanoparticles by template-assisted combustion method. *Mater. Manuf. Processes* 27 (9), 901–904. <https://doi.org/10.1080/10426914.2011.610086>.
- He, H.-Y., 2013. Structural and magnetic property of $\text{Co}_{1-x}\text{Ni}_x\text{Fe}_2\text{O}_4$ nanoparticles synthesized by hydrothermal method. *Int. J. Appl. Ceram. Technol.* 11 (4), 626–636. <https://doi.org/10.1111/ijac.12071>.
- Heiba, Z.K., Mostafa, N.Y., Abd-Elkader, O.H., 2014. Structural and magnetic properties correlated with cation distribution of Mo-substituted cobalt ferrite nanoparticles. *J. Magn. Mater.* 368, 246–251. <https://doi.org/10.1016/j.jmmm.2014.05.036>.
- Horcas, I., Fernández, R., Gómez-Rodríguez, J.M., Colchero, J., Gómez-Herrero, J., Baro, A.M., 2007. WSXM: a software for scanning probe microscopy and a tool for nanotechnology. *Rev. Sci. Instrum.* 78, (1). <https://doi.org/10.1063/1.2432410>
- Huixia, F., Baiyi, C., Deyi, Z., Jianqiang, Z., Lin, T., 2014. Preparation and characterization of the cobalt ferrite nano-particles by reverse coprecipitation. *J. Magn. Mater.* 356, 68–72. <https://doi.org/10.1016/j.jmmm.2013.12.033>.
- Hutamaningtyas, E., Utari, Suharyana, Purnama, B., Wijayanta, A.T., 2016. Effects of the synthesis temperature on the crystalline structure and the magnetic properties of cobalt ferrite nanoparticles prepared by coprecipitation. *J. Korean Phys. Soc.* 69 (4), 584–588. <https://doi.org/10.3938/jkps.69.584>.
- Huang, X., Zhang, J., Wang, W., Sang, T., Song, B., Zhu, H., Rao, W., Wong, C., 2016. Effect of pH value on electromagnetic loss properties of Co–Zn ferrite prepared via coprecipitation method. *J. Magn. Mater.* 405, 36–41. <https://doi.org/10.1016/j.jmmm.2015.12.051>.
- Kefeni, K.K., Msagati, T.A., Mamba, B.B., 2017. Ferrite nanoparticles: synthesis, characterisation and applications in electronic device. *Mater. Sci. Eng., B* 215, 37–55. <https://doi.org/10.1016/j.mseb.2016.11.002>.

- Kotnala, R.K., Shah, J., 2015. Ferrite materials. In: Handbook of Magnetic Materials. pp. 291–379. doi:10.1016/b978-0-444-63528-0.00004-8.
- Kumar, R., Kar, M., 2016. Lattice strain induced magnetism in substituted nanocrystalline cobalt ferrite. *J. Magn. Magn. Mater.* 416, 335–341. <https://doi.org/10.1016/j.jmmm.2016.05.035>.
- Lima, A.C., Peres, A.P.S., Araújo, J.H., Morales, M.A., Medeiros, S.N., Soares, J.M., Melo, D.M.A., Carriço, A.S., 2015. The effect of Sr^{2+} on the structure and magnetic properties of nanocrystalline cobalt ferrite. *Mater. Lett.* 145, 56–58. <https://doi.org/10.1016/j.matlet.2015.01.066>.
- Liu, M., Lu, M., Wang, L., Xu, S., Zhao, J., Li, H., 2016. Mössbauer study on the magnetic properties and cation distribution of $CoFe_2O_4$ nanoparticles synthesized by hydrothermal method. *J. Mater. Sci.* 51 (11), 5487–5492. <https://doi.org/10.1007/s10853-016-9853-3>.
- Maaz, K., Mumtaz, A., Hasanain, S.K., Ceylan, A., 2007. Synthesis and magnetic properties of cobalt ferrite ($CoFe_2O_4$) nanoparticles prepared by wet chemical route. *J. Magn. Magn. Mater.* 308 (2), 289–295. <https://doi.org/10.1016/j.jmmm.2006.06.003>.
- Manikandan, A., Kennedy, L.J., Bououdina, M., Vijaya, J.J., 2014. Synthesis, optical and magnetic properties of pure and Co-doped $ZnFe_2O_4$ nanoparticles by microwave combustion method. *J. Magn. Magn. Mater.* 349, 249–258. <https://doi.org/10.1016/j.jmmm.2013.09.013>.
- Maurya, J.C., Janrao, P.S., Datar, A.A., Kanhe, N.S., Bhoraskar, S.V., Mathe, V.L., 2016. Evidence of domain wall pinning in aluminum substituted cobalt ferrites. *J. Magn. Magn. Mater.* 412, 164–171. <https://doi.org/10.1016/j.jmmm.2016.03.074>.
- Mahmoud, M.H., Elshahawy, A.M., Makhlof, S.A., Hamdeh, H.H., 2014. Synthesis of highly ordered 30 nm $NiFe_2O_4$ particles by the microwave-combustion method. *J. Magn. Magn. Mater.* 369, 55–61. <https://doi.org/10.1016/j.jmmm.2014.06.011>.
- Mohamed, M.B., Yehia, M., 2014. Cation distribution and magnetic properties of nanocrystalline gallium substituted cobalt ferrite. *J. Alloys Compd.* 615, 181–187. <https://doi.org/10.1016/j.jallcom.2014.06.156>.
- Monaji, V.R., Indla, S., Rayaprol, S., Sowmya, S., Srinivas, A., Das, D., 2017. Temperature dependent magnetic properties of $Co_{1+x}Ti_xFe_{2-2x}O_4$ ($T = Zr, Ti$). *J. Alloys Compd.* 700, 92–97. <https://doi.org/10.1016/j.jallcom.2017.01.061>.
- Nlebedim, I.C., Melikhov, Y., Jiles, D.C., 2014. Temperature dependence of magnetic properties of heat treated cobalt ferrite. *J. Appl. Phys.* 115, (4). <https://doi.org/10.1063/1.4862300> 043903.
- Nlebedim, I.C., Jiles, D.C., 2015. Thermal effects on the magnetic properties of titanium modified cobalt ferrite. *J. Appl. Phys.* 117 (17), 17A506. <https://doi.org/10.1063/1.4919229>.
- Prabhakaran, T., Mangalaraja, R.V., Denardin, J.C., Jiménez, J.A., 2017a. The effect of reaction temperature on the structural and magnetic properties of nano $CoFe_2O_4$. *Ceram. Int.* 43 (7), 5599–5606. <https://doi.org/10.1016/j.ceramint.2017.01.092>.
- Prabhakaran, T., Mangalaraja, R.V., Denardin, J.C., Jiménez, J.A., 2017b. The effect of calcination temperature on the structural and magnetic properties of co-precipitated $CoFe_2O_4$ nanoparticles. *J. Alloys Compd.* 716, 171–183. <https://doi.org/10.1016/j.jallcom.2017.05.048>.
- Purnama, B., Rahmawati, R., Wijayanta, A.T., Suharyana, S., 2015. Dependence of structural and magnetic properties on annealing times in Co-precipitated cobalt ferrite nanoparticles. *J. Magn.* 20 (3), 207–210. <https://doi.org/10.4283/jmag.2015.20.3.207>.
- Rakshit, R., Mandal, M., Pal, M., Mandal, K., 2014. Tuning of magnetic properties of $CoFe_2O_4$ nanoparticles through charge transfer effect. *Appl. Phys. Lett.* 104, (9). <https://doi.org/10.1063/1.4867706> 092412.
- Safi, R., Ghasemi, A., Shoja-Razavi, R., Tavousi, M., 2015. The role of pH on the particle size and magnetic consequence of cobalt ferrite. *J. Magn. Magn. Mater.* 396, 288–294. <https://doi.org/10.1016/j.jmmm.2015.08.022>.
- Saidani, M., Belkacem, W., Bezerghéanu, A., Cizmas, C.B., Mliki, N., 2015. *J. Alloys Compd.* 653, 513–522. <https://doi.org/10.1016/j.jallcom.2015.09.020>.
- Sato Turtelli, R., Atif, M., Mehmood, N., Kubel, F., Biernacka, K., Linert, W., Grössinger, R., Kapusta, C., Sikora, M., 2012. Interplay between the cation distribution and production methods in cobalt ferrite. *Mater. Chem. Phys.* 132 (2–3), 832–838. <https://doi.org/10.1016/j.matchemphys.2011.12.020>.
- Shirsath, S.E., Liu, X., Yasukawa, Y., Li, S., Morisako, A., 2016. Switching of magnetic easy-axis using crystal orientation for large perpendicular coercivity in $CoFe_2O_4$ thin film. *Sci. Rep.* 6, 30074. <https://doi.org/10.1038/srep30074>.
- Swatsitang, E., Phokha, S., Hunpratub, S., Usher, B., Bootchanont, A., Maensiri, S., Chindaprasit, P., 2016. Characterization and magnetic properties of cobalt ferrite nanoparticles. *J. Alloys Compd.* 664, 792–797. <https://doi.org/10.1016/j.jallcom.2015.12.230>.
- Tang, X., Jin, L., Chen, F., Wei, R., Yang, J., Dai, J., Song, W., Zhu, X., Sun, Y., 2016. Dwell time effects on high coercivity $CoFe_2O_4$ thin films deposited by the solution processing. *Appl. Phys. Lett.* 109, (15). <https://doi.org/10.1063/1.4964836> 152406.
- Tang, X., Jin, L., Wei, R., Zhu, X., Yang, J., Dai, J., Song, W., Zhu, X., Sun, Y., 2017. High-coercivity $CoFe_2O_4$ thin films on Si substrates by sol-gel. *J. Magn. Magn. Mater.* 422, 255–261. <https://doi.org/10.1016/j.jmmm.2016.09.022>.
- Yadav, R.S., Havlica, J., Hnatko, M., Šajgalik, P., Alexander, C., Palou, M., Bartoničková, E., Boháč, M., Frajkorová, F., Masilko, J., Zmrzljý, M., Kalina, L., Hajdúchová, M., Enev, V., 2015. Magnetic properties of $Co_{1-x}Zn_xFe_2O_4$ spinel ferrite nanoparticles synthesized by starch-assisted sol-gel autocombustion method and its ball milling. *J. Magn. Magn. Mater.* 378, 190–199. <https://doi.org/10.1016/j.jmmm.2014.11.027>.
- Zaki, H.M., Al-Heniti, S.H., Hashhash, A., 2015. Effect of Al^{3+} ion addition on the magnetic properties of cobalt ferrite at moderate and low temperatures. *J. Magn. Magn. Mater.* 401, 1027–1032. <https://doi.org/10.1016/j.jmmm.2015.11.021>.
- Zhao, L., Zhang, H., Xing, Y., Song, S., Yu, S., Shi, W., Guo, X., Yang, J., Lei, Y., Cao, F., 2008. Studies on the magnetism of cobalt ferrite nanocrystals synthesized by hydrothermal method. *J. Solid State Chem.* 181 (2), 245–252. <https://doi.org/10.1016/j.jssc.2007.10.034>.